CHEMISTRY
AN ASIAN JOURNAL

DOI: 10.1002/asia.200600184

Kinetic Studies Prove High Catalytic Activity of a Diene–Rhodium Complex in 1,4-Addition of Phenylboronic Acid to α,β-Unsaturated Ketones

Asato Kina,[a] Yuichi Yasuhara,[a] Takahiro Nishimura,[a] Hiroshi Iwamura,[b] and Tamio Hayashi*[a]

Abstract: In the 1,4-addition of phenylboronic acid to α,β-unsaturated ketones, $[Rh(OH)(cod)]_2$ has a much higher catalytic activity than $[Rh(OH)(binap)]_2$ (cod = 1,5-cyclooctadiene, binap = 2,2′-bis(diphenylphosphanyl)-1,1′-binaphthyl). Kinetic studies revealed that the rate-determining transmetalation step in the catalytic cycle has a large rate constant when $[Rh(OH)(cod)]_2$ is used.

Keywords: addition · catalytic cycles · diene ligands · kinetics · rhodium

Introduction

The outcome of asymmetric reactions catalyzed by metal complexes is strongly dependent on the chiral ligands.[1] The use of 2,2′-bis(diphenylphosphanyl)-1,1′-binaphthyl (binap)[2] as a chiral ligand has made the rhodium-catalyzed asymmetric 1,4-addition of organoboron reagents to electron-deficient olefins one of the most-efficient methods of asymmetric carbon–carbon bond formation.[3–5] The chiral diene ligands, which we reported for the first time in 2003, improved this rhodium-catalyzed asymmetric addition in terms of both catalytic activity and enantioselectivity.[6] Several types of chiral diene ligands have been prepared and applied successfully to asymmetric 1,4-addition to α,β-unsaturated carbonyl compounds,[7,8] asymmetric 1,2-addition to *N*-sulfonylarylimines,[9] and arylative cyclization of alkynes that bear an aldehyde or enoate moiety.[10] In these reactions, the most significant feature of the rhodium–diene system is its high catalytic activity. For example, 0.005–0.01 mol% of a rhodium complex coordinated with (*S*,*S*)-2,5-dibenzylbicyclo[2.2.2]octa-2,5-diene (Bn-bod*) can catalyze asymmetric 1,4-addition in high yields without loss of enantioselectivity.[11] Our recent kinetic studies on 1,4-addition catalyzed by a binap–rhodium complex[12] determined the kinetic parameters within the catalytic cycle and revealed that the reaction is characterized by a) the predominant catalytic inactive dimeric species $[Rh(OH)(binap)]_2$ and b) a rate-determining transmetalation step (Scheme 1). To determine the reasons for the big difference in catalytic activity between diene–rhodium and phosphine–rhodium complexes, we also studied the kinetics of the reaction catalyzed by a diene–rhodium complex. Herein we report the kinetic features of the diene–rhodium system in comparison with the binap–rhodium system.

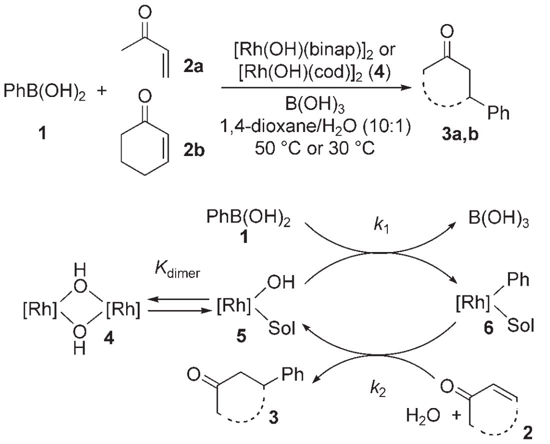

Scheme 1. Rhodium-catalyzed 1,4-addition of phenylboronic acid (**1**) to enones **2** and its mechanism. cod = 1,5-Cyclooctadiene, [Rh] = Rh(binap) or Rh(cod), Sol = solvent.

---

[a] A. Kina, Y. Yasuhara, Dr. T. Nishimura, Prof. Dr. T. Hayashi
Department of Chemistry
Graduate School of Science, Kyoto University
Sakyo, Kyoto 606-8502 (Japan)
Fax: (+81) 75-753-3988
E-mail: thayashi@kuchem.kyoto-u.ac.jp

[b] H. Iwamura
Mitsubishi Pharma Corporation
Kamitsu, Ibaraki 314-0255 (Japan)

Supporting information for this article is available on the WWW under http://www.chemasianj.org or from the author.

Results and Discussion

As a rhodium catalyst coordinated with diene ligands, $[Rh(OH)(cod)]_2$ (**4**) was chosen because it can be readily obtained in large quantities[13] and is known to show high catalytic activity for 1,4-addition.[14] The reactions of phenylboronic acid ($PhB(OH)_2$; **1**)[15] with methyl vinyl ketone (MVK; **2a**) in aqueous dioxane in the presence of **4** and boric acid[16] at 50 or 30 °C (Scheme 1) were carried out in a reaction calorimeter (Omnical SuperCRC) for continuous monitoring over the course of the reaction; the significant point is the use of an excess amount of **2a** to prevent any **1** from remaining. The kinetic data were analyzed by reaction-progress kinetic analysis, which was developed by Blackmond and co-workers.[17,18] The experimental procedures were similar to those used for the previous kinetic studies on the binap system.[12]

In the first set of experiments, the catalytic activity of **4** was compared with that of $[Rh(OH)(binap)]_2$ in the reaction of **1** with **2a** at 50 °C. The results obtained with $[Rh]_{total} = 1.30$ mM showed that the diene complex **4** is about 20 times more active than the binap complex (Figure 1). Thus, for 50 % conversion of **1**, it takes only 3 min with **4** compared to 50 min with $[Rh(OH)(binap)]_2$.

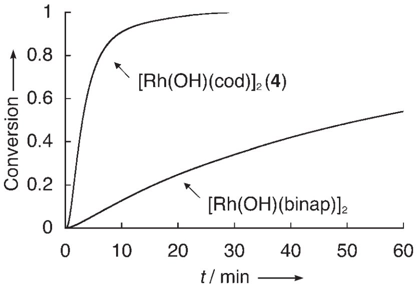

Figure 1. Conversion versus time curves for the reactions of **1** ($[\mathbf{1}]_0 = 69$ mM) with **2a** ($[\mathbf{2a}]_0 = 100$ mM) in 1,4-dioxane (6.0 mL) and H_2O (0.6 mL) in the presence of rhodium catalyst ($[Rh]_{total} = 1.30$ mM Rh) and $[B(OH)_3]_0 = 533$ mM at 50 °C. The rhodium catalysts used for the reactions were $[Rh(OH)(cod)]_2$ (**4**) and $[Rh(OH)(binap)]_2$.

For further experiments to obtain kinetic parameters in the reaction with **4** as a catalyst, we chose 2.70 mM for the total Rh concentration and 30 °C for the reaction temperature as standard reaction conditions. In our previous kinetic studies with $[Rh(OH)(binap)]_2$ catalyst, they were 8.00 mM and 50 °C, respectively.[12] In the present Rh/diene system, the catalyst concentration is lower because of the higher catalytic activity, and the reaction temperature is lower to avoid the low accuracy caused by high temperature (see below). The concentration of **1** was plotted as the x axis and the reaction rate as the y axis (Figure 2). The two curves for the reactions carried out at the same ["excess"][19] (i.e., the difference in the initial concentrations of the two substrates) overlaid well, revealing that the system suffers from neither catalyst deactivation nor product inhibition (Figure 2a and b). The order of the reaction with respect to the catalyst was determined to be 0.65, which is demonstrated by the overlapping plot of reaction rate divided by $[Rh]_{total}^{0.65}$ versus the concentration of **1** (Figure 2, inset). This reaction order (0.65) for the catalyst indicates that the inactive dimeric hydroxorhodium complex **4** is a dominant species in the catalytic cycle.[20] However, in contrast to the previous binap–rhodium system,[12] in which the order with respect to the catalyst is nearly 0.5 [Eq. (1)], it also indicates that the concentration of the monomeric hydroxorhodium species **5** is no longer negligible, and as a result, Equation (1) is not an appropriate simplified expression in the present diene–rhodium system. The results of the reactions carried out at different ["excess"][19] (Figure 2a, c, d, and e) showed that the reaction is first-order with respect to **1** and zero-order with respect to **2a**. It follows that the rate-determining step is the formation of the phenyl–rhodium species **6** and that the following insertion step is fast. When k_2[MVK] is much larger than $k_1[PhB(OH)_2]$ due to the excess amount of MVK (**2a**) and the large value for the rate constant k_2 (described in detail below), the full expression of the rate equation [Eq. (2)] approaches Equation (3), which does not include the rate constant for the insertion k_2 but allows us to extract accurate values independently for the rate constant for the transmetalation k_1 and the dimerization constant K_{dimer}.[12] As shown by the straight lines in Figure 2, analysis of the progress of the reaction during 30–90 % conversion after the induction period revealed a good fit to Equation (3) when $k_1 = 1.3\,M^{-1}s^{-1}$ and $K_{dimer} = 3.8 \times 10^2\,M^{-1}$ (standard deviations 1 % and 3 %, respectively).[21] The rate constant k_1 at 30 °C is two times larger than that with the binap–rhodium catalyst at 50 °C.

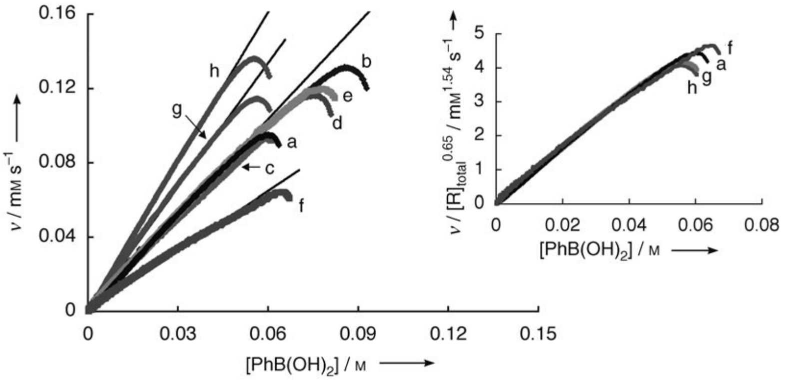

Figure 2. Rate versus [**1**] and rate/$[Rh]^{0.65}$ versus [**1**] (inset) curves for the reactions of **1** with **2a** in 1,4-dioxane (3.0 mL) and H_2O (0.3 mL) in the presence of **4** with $[B(OH)_3]_0 = 536$ mM at 30 °C. Reaction conditions: a) $[\mathbf{1}]_0 = 67.9$ mM, $[\mathbf{2a}]_0 = 201$ mM, $[Rh] = 2.70$ mM Rh; b) $[\mathbf{1}]_0 = 98.5$ mM, $[\mathbf{2a}]_0 = 234$ mM, $[Rh] = 2.66$ mM Rh; c) $[\mathbf{1}]_0 = 66.0$ mM, $[\mathbf{2a}]_0 = 128$ mM, $[Rh] = 2.60$ mM Rh; d) $[\mathbf{1}]_0 = 85.6$ mM, $[\mathbf{2a}]_0 = 200$ mM, $[Rh] = 2.73$ mM Rh; e) $[\mathbf{1}]_0 = 88.6$ mM, $[\mathbf{2a}]_0 = 110$ mM, $[Rh] = 2.73$ mM Rh; f) $[\mathbf{1}]_0 = 70.4$ mM, $[\mathbf{2a}]_0 = 200$ mM, $[Rh] = 1.37$ mM Rh; g) $[\mathbf{1}]_0 = 65.8$ mM, $[\mathbf{2a}]_0 = 198$ mM, $[Rh] = 3.97$ mM Rh; h) $[\mathbf{1}]_0 = 65.8$ mM, $[\mathbf{2a}]_0 = 198$ mM, $[Rh] = 5.33$ mM Rh.

$$v = \frac{k_1}{\sqrt{2K_{\text{dimer}}}}[\text{PhB(OH)}_2(\mathbf{1})][\text{Rh}]_{\text{total}}{}^{0.5} \tag{1}$$

$$v = \frac{2k_1k_2[\text{PhB(OH}_2)(\mathbf{1})][\text{enone}(\mathbf{2})][\text{Rh}]_{\text{total}}}{A + \sqrt{A^2 + 8K_{\text{dimer}}(k_2[\text{enone}(\mathbf{2})])^2[\text{Rh}]_{\text{total}}}}, \tag{2}$$

$$A = k_1[\text{PhB(OH)}_2(\mathbf{1})] + k_2[\text{enone}(\mathbf{2})]$$

$$v = \frac{2k_1[\text{PhB(OH}_2)(\mathbf{1})][\text{Rh}]_{\text{total}}}{1 + \sqrt{1 + 8K_{\text{dimer}}[\text{Rh}]_{\text{total}}}} \tag{3}$$

It is desirable to compare k_1 in the diene system with that in the binap system at the same temperature. Unfortunately, determination of statistically certain values for the diene system at 50 °C failed owing to slight catalyst deactivation and inadequate data points caused by too high a reaction rate. We assumed that K_{dimer} at 50 °C has a similar value ($K_{\text{dimer}} = 3.8 \times 10^2\,\text{M}^{-1}$) to that at 30 °C, because the reaction order with respect to the catalyst at 50 °C is 0.65, which is the same value as at 30 °C. By substituting this K_{dimer} value in Equation (3), k_1 at 50 °C was estimated to be $6.7\,\text{M}^{-1}\text{s}^{-1}$ from the fit of the experimental rate data (Figure 3) to Equation (3). This estimated k_1 value allows us to make a quantitative comparison between the diene and binap systems at 50 °C (Table 1). Whereas the dimerization constant for the cod complex ($K_{\text{dimer}} = 3.8 \times 10^2\,\text{M}^{-1}$) is not very different from that for the binap complex ($K_{\text{dimer}} = 8 \times 10^2\,\text{M}^{-1}$), the rate constant k_1 for the cod catalyst ($k_1 = 6.7\,\text{M}^{-1}\text{s}^{-1}$) is more than 10 times larger than that for the binap catalyst ($k_1 = 0.5\,\text{M}^{-1}\text{s}^{-1}$).[12] Such a large rate constant k_1 brings about the high catalytic activity observed in the reactions with the diene ligand.

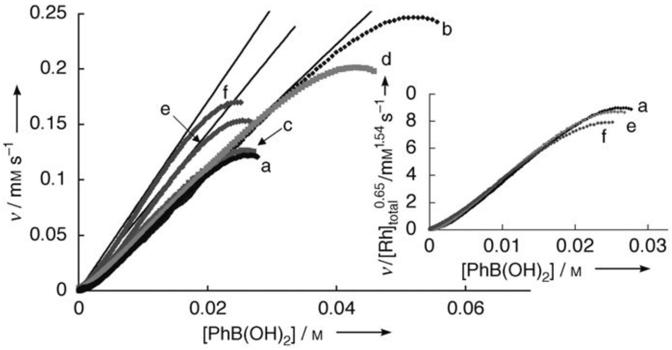

Figure 3. Rate versus [**1**] for the reactions of **1** with **2a** in 1,4-dioxane (6.0 mL) and H_2O (0.6 mL) in the presence of **4** with $[\text{B(OH)}_3]_0 = 533$ mM at 50 °C. Reaction conditions: a) $[\mathbf{1}]_0 = 33.5$ mM, $[\mathbf{2a}]_0 = 67.0$ mM, [Rh] = 1.34 mM Rh; b) $[\mathbf{1}]_0 = 67.0$ mM, $[\mathbf{2a}]_0 = 101$ mM, [Rh] = 1.34 mM Rh; c) $[\mathbf{1}]_0 = 33.5$ mM, $[\mathbf{2a}]_0 = 101$ mM, [Rh] = 1.33 mM Rh; d) $[\mathbf{1}]_0 = 55.5$ mM, $[\mathbf{2a}]_0 = 101$ mM, [Rh] = 1.36 mM Rh; e) $[\mathbf{1}]_0 = 33.5$ mM, $[\mathbf{2a}]_0 = 67.0$ mM, [Rh] = 2.00 mM Rh; f) $[\mathbf{1}]_0 = 33.5$ mM, $[\mathbf{2a}]_0 = 67.0$ mM, [Rh] = 2.71 mM Rh.

Table 1. Rate and equilibrium constants determined by fitting of the experimental data of Figures 2 and 3 to Equation (3).[a]

	Rh/cod 30 °C	Rh/cod 50 °C	Rh/binap[b] 50 °C
k_1 [$\text{M}^{-1}\text{s}^{-1}$]	1.3 (1)	6.7	0.5
K_{dimer} [M^{-1}]	3.8×10^2 (3)	[3.8×10^2][c]	8×10^2

[a] The values in parentheses are the standard deviations. [b] The results for Rh/binap system are reported in reference [12]. [c] Assumed value.

It is difficult to determine the rate constant k_2 for the insertion step, because it is too fast to affect the overall reaction rate. To observe the influence of the insertion, k_2[enone] should not be much larger than $k_1[\text{PhB(OH)}_2]$ in the full expression of Equation (2). Thus, when the concentration of the enone **2** becomes much lower than that of PhB(OH)_2 (**1**), Equation (2) allows us to determine k_2. The reaction of **1** (97 mM) with a smaller amount of 2-cyclohexenone (**2b**; 46 mM), in which the ratio of **1** to **2** is opposite to that used for the measurement of k_1, exhibited a characteristic shoulder in the heat flow versus time curve (Figure 4 a); the curve falls as the concentration of **2b** is lowered. Before the shoulder (highlighted), it overlaps with the curve for the reaction with an excess amount of **2b** (231 mM). However, the heat flow was not complete after the consumption of **2b** (around 10 min); a further heat flow was observed, producing a sharp bend in the curve. This indicates that 1,4-addition to **2b** proceeds at first, then the hydrolysis of **1** to give benzene begins as the concentration of **2b** approaches 0 mM, which was confirmed by the exact overlay between the heat-flow curve after 10 min and that of hydrolysis of the remaining amount of **1** (51 mM = (97−46) mM). The heat flow for the 1,4-addition, which was obtained by subtraction of the heat flow of the hydrolysis from the total heat flow, enabled us to plot the reaction rate against the concentration of **1**. The rate constant k_2 of **2b** was estimated to be $16\,\text{M}^{-1}\text{s}^{-1}$ by fitting to Equation (2) with

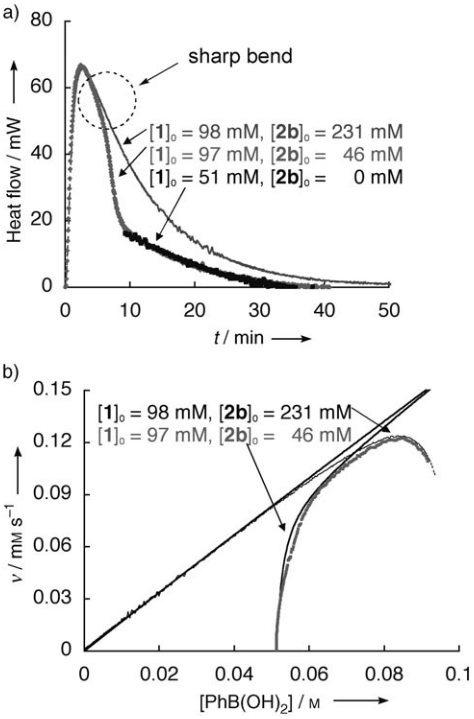

Figure 4. a) Heat flow versus time and b) rate versus [**1**] curves for the reactions of **1** with **2b** in 1,4-dioxane (3.0 mL) and H_2O (0.3 mL) in the presence of **4** (2.70 mM Rh) with $[\text{B(OH)}_3]_0 = 533$ mM at 30 °C.

$k_1 = 1.3\,\text{M}^{-1}\text{s}^{-1}$ and $K_\text{dimer} = 3.8\times10^2\,\text{M}^{-1}$ (Figure 4b, solid lines). The k_1 and K_dimer values obtained for **2b** were identical to those for **2a** obtained in a similar manner with Equation (3). This large value for the insertion of **2b** is consistent with the approximation used for Equation (3). Unfortunately, it was difficult to obtain satisfactory data in the case of **2a** owing to the remarkably fast insertion of **2a** relative to **2b**. We believe that there was too rapid a change in heat flow at the final stage of the reaction for reaction calorimetry to respond. Actually, the reaction of **1** with **2a** (1 equiv) and **2b** (1 equiv) in competition in the presence of **4** resulted in exclusive formation of the 1,4-addition product **3a**, which is derived from the more-reactive **2a** (>100:1; ^{1}H NMR spectroscopic analysis). This is in good agreement with the extremely fast insertion of **2a**.

Conclusions

In summary, we have carried out kinetic studies of the 1,4-addition of phenylboronic acid (**1**) to α,β-unsaturated ketones **2** in the presence of a rhodium complex coordinated with 1,5-cyclooctadiene by utilizing reaction calorimetry. The reaction mechanism of the diene system was found to be similar to that of the binap system, and the inactive dimeric species **4** is the resting state. The remarkably high catalytic activity of diene–rhodium is attributed to a large rate constant for the rate-determining transmetalation step.

Experimental Section

General

All anaerobic and moisture-sensitive manipulations were carried out with standard Schlenk techniques under predried nitrogen or with glovebox techniques under prepurified argon. NMR spectra were recorded at 500 MHz for ^{1}H, 125 MHz for ^{13}C, and 202 MHz for ^{31}P. Chemical shifts are reported in ppm referenced to internal $SiMe_4$ (phosphoric acid for ^{31}P NMR spectroscopy). 1,4-Dioxane was distilled over benzophenone ketyl under N_2. 1,4-Dioxane and H_2O were degassed by bubbling of N_2. Both **2a** and **2b** were distilled before use from $CaCl_2$. Phenylboroxine[11] and **4**[13] were prepared according to the reported procedures. Boric acid ($B(OH)_3$) was used as received. The synthesis of the 1,4-addition products, 4-phenyl-2-butanone (**3a**; CAS 2550-26-7) and 3-phenylcyclohexanone (**3b**; CAS 20795-53-3), have already been reported.

Experimental Procedure for Kinetic Studies with Reaction Calorimetry

Reactions were performed in an Omnical SuperCRC reaction calorimeter. The instrument contains a differential scanning calorimeter (DSC), which compares the heat released or consumed in a sample vessel to that in a reference vessel. The reaction vessels were borosilicate screw-thread vials (16 mL) fitted with open-top black phenolic screw caps and white polytetrafluoroethylene (PTFE) septa charged with teflon stirrer bars. Sample volumes did not exceed 7 mL. In a typical calorimetry experiment, 1,4-dioxane (5.0 mL) and H_2O (0.5 mL) were added to a reaction vessel containing **4** (2.06 mg, 9.00 μmol) and $B(OH)_3$ (222 mg, 3.6 mmol). The vessel was placed in the calorimeter, and the mixture was stirred for over 30 min to allow the contents of the vessel to reach thermal equilibrium. A vessel that contained the same chemicals but without **4** was prepared as the reference vessel. A syringe containing substrate solution (1.15 mL of a solution of phenylboroxine (70.1 mg, 0.674 mmol) and **2a** (143 mg, 2.04 mmol) in 1,4-dioxane (3.0 mL) and H_2O (0.30 mL)) was placed in the sample-injection ports of the calorimeter for the reaction and reference vessels. These two syringes were allowed to equilibrate thermally. The reaction was initiated by injecting the substrate solution into the reaction vessel; the same substrate solution was injected into the reference vessel simultaneously to remove any thermal differences. The temperature of the DSC was held constant at 50 °C with a Titec CL-150F water circulator to ensure that the reactions proceeded under isothermal conditions. A raw-data curve was produced by measuring the heat flow from the sample vessel every three seconds during the reaction. Owing to the delay between the moment heat was evolved from the reaction vessel and the time when the heat flow was detected by the thermophile sensor, the raw-data curve had to be calibrated. For the calibration, a constant current was passed through a resistor in the sample chamber of the calorimeter, thereby producing a known quantity of heat. This process resulted in a response curve, which was then transformed into a square wave, allowing the response time of the instrument to be calculated with WinCRC software. Application of the response time to the raw data resulted in a "tau-corrected data curve", a plot of heat flow ($\text{mJ}\,\text{s}^{-1}$) versus time. The reaction rate, which is directly proportional to the heat flow [Eq. (4)], fraction conversion [Eq. (5)], and instantaneous concentrations of reactants/products can all be calculated from this tau-corrected data curve:

$$q = \Delta H_\text{r} V \nu \tag{4}$$

where q is the reaction heat flow, ΔH_r is the enthalpy change of reaction, V is the reaction volume, and ν is the reaction rate. The enthalpy change of reaction from integration of the observed heat flow versus time curves gave an average value of $(162\pm8)\,\text{kJ}\,\text{mol}^{-1}$:

$$\text{conversion} = \frac{\int_0^t q(t)\text{d}t}{\int_0^{tf} q(t)\text{d}t} \tag{5}$$

where the numerator represents the area under the heat flow curve up to any time point t, and the denominator represents the total area under the heat flow curve.

The reaction was also monitored by NMR spectroscopic analysis, for which the samples were prepared by diluting the reaction mixture (40 μL) with $CDCl_3$ (0.5 mL). It was confirmed by NMR spectroscopic analysis that the generation of benzene by hydrolysis of **1** is less than 3 %. The conversion measured by NMR spectroscopy was in good agreement with that measured by heat flow (see Supporting Information), thus validating the use of reaction calorimetry to follow the Rh/cod-catalyzed 1,4-addition of **1**.

Kinetic Model for α,β-Unsaturated Ketones with Rh/Cod Catalyst

The rate of formation of product **3** is given by [Eq. (6)]:

$$\nu = k_2[\mathbf{6}][\mathbf{2}] \tag{6}$$

The concentration of each catalyst species is related by material balance to the total rhodium concentration in [Eq. (7)]:

$$[\text{Rh}]_\text{total} = 2[\mathbf{4}] + [\mathbf{5}] + [\mathbf{6}] \tag{7}$$

The equilibrium constant K_dimer is defined as an association rather than a dissociation constant in [Eq. (8)]:

$$K_\text{dimer} = \frac{[\mathbf{4}]}{[\mathbf{5}]^2} \tag{8}$$

The steady-state equation for **6** is given by [Eq. (9)]:

$$\begin{aligned} \frac{\text{d}[\mathbf{6}]}{\text{d}t} &= k_1[\mathbf{1}][\mathbf{5}] - k_2[\mathbf{2}][\mathbf{6}] = 0 \\ [\mathbf{5}] &= \frac{k_2[\mathbf{2}]}{k_1[\mathbf{1}]}[\mathbf{6}] \end{aligned} \tag{9}$$

Substituting [**5**] into [Eq. (8)] gives [Eq. (10)]:

$$[\mathbf{4}] = K_{\text{dimer}}[\mathbf{5}]^2 = K_{\text{dimer}}\left(\frac{k_2[\mathbf{2}]}{k_1[\mathbf{1}]}\right)^2[\mathbf{6}]^2 \tag{10}$$

Combining [Eq. (9)] and [Eq. (10)] with [Eq. (7)] gives [Eq. (11)]:

$$\begin{aligned}&[\text{Rh}]_{\text{total}} = 2K_{\text{dimer}}\left(\frac{k_2[\mathbf{2}]}{k_1[\mathbf{1}]}\right)^2[\mathbf{6}]^2 + \frac{k_2[\mathbf{2}]}{k_1[\mathbf{1}]}[\mathbf{6}] + [\mathbf{6}]\\ &[\mathbf{6}] = \frac{2k_1[\mathbf{1}][\text{Rh}]_{\text{total}}}{(k_1[\mathbf{1}]+k_2[\mathbf{2}]) + \sqrt{(k_1[\mathbf{1}]+k_2[\mathbf{2}])^2 + 8K_{\text{dimer}}(k_2[\mathbf{2}])^2[\text{Rh}]_{\text{total}}}}\end{aligned} \tag{11}$$

Substituting [**6**] into [Eq. (6)] gives [Eq. (12)] for the rate of product formation:

$$v = \frac{2k_1k_2[\mathbf{1}][\mathbf{2}][\text{Rh}]_{\text{total}}}{(k_1[\mathbf{1}]+k_2[\mathbf{2}]) + \sqrt{(k_1[\mathbf{1}]+k_2[\mathbf{2}])^2 + 8K_{\text{dimer}}(k_2[\mathbf{2}])^2[\text{Rh}]_{\text{total}}}} \tag{12}$$

Transformation 1: When $K_{\text{dimer}}[\text{Rh}]_{\text{total}}$ is large, the reaction rate will show first-order kinetics with respect to **1** and half-order kinetics with respect to Rh_{total}, as shown in [Eq. (13)]:

$$v = \frac{k_1}{\sqrt{2K_{\text{dimer}}}}[\mathbf{1}][\text{Rh}]_{\text{total}}^{0.5} \tag{13}$$

Transformation 2: At first, both the numerator and denominator are divided by $k_2[\mathbf{2}]$, [Eq. (14)]:

$$v = \frac{2k_1[\mathbf{1}][\text{Rh}]_{\text{total}}}{\left(1+\frac{k_1[\mathbf{1}]}{k_2[\mathbf{2}]}\right) + \sqrt{\left(1+\frac{k_1[\mathbf{1}]}{k_2[\mathbf{2}]}\right)^2 + 8K_{\text{dimer}}[\text{Rh}]_{\text{total}}}} \tag{14}$$

When $k_2[\mathbf{2}]$ is much larger than $k_1[\mathbf{1}]$, the rate equation is reduced to [Eq. (3)], which no longer includes the large rate constant for the insertion:

$$v = \frac{2k_1[\mathbf{1}][\text{Rh}]_{\text{total}}}{1 + \sqrt{1 + 8K_{\text{dimer}}[\text{Rh}]_{\text{total}}}} \tag{3}$$

Transformation 3: Next, both the numerator and denominator are divided by $k_1[\mathbf{1}]$, [Eq. (15)]:

$$v = \frac{2k_2[\mathbf{2}][\text{Rh}]_{\text{total}}}{\left(1+\frac{k_2[\mathbf{2}]}{k_1[\mathbf{1}]}\right) + \sqrt{\left(1+\frac{k_2[\mathbf{2}]}{k_1[\mathbf{1}]}\right)^2 + 8K_{\text{dimer}}\left(\frac{k_2[\mathbf{2}]}{k_1[\mathbf{1}]}\right)^2[\text{Rh}]_{\text{total}}}} \tag{15}$$

When $k_1[\mathbf{1}]$ is much larger than $k_2[\mathbf{2}]$, the rate equation is simplified to [Eq. (16)]:

$$v = k_2[\mathbf{2}][\text{Rh}]_{\text{total}} \tag{16}$$

Acknowledgements

Support was provided in part by a Grant-in-Aid for Scientific Research from the Ministry of Education, Culture, Sports, Science, and Technology, Japan (21 COE on Kyoto University Alliance for Chemistry).

---

[1] For reviews, see: a) *Comprehensive Asymmetric Catalysis* (Eds.: E. N. Jacobsen, A. Pfaltz, H. Yamamoto), Springer, Heidelberg, **1999**; b) *Catalytic Asymmetric Synthesis*, *2nd ed.* (Ed.: I. Ojima), Wiley, New York, **2000**.

[2] A. Miyashita, A. Yasuda, H. Takaya, K. Toriumi, T. Ito, T. Souchi, R. Noyori, *J. Am. Chem. Soc.* **1980**, *102*, 7932.

[3] Y. Takaya, M. Ogasawara, T. Hayashi, M. Sakai, N. Miyaura, *J. Am. Chem. Soc.* **1998**, *120*, 5579.

[4] For reviews, see: a) T. Hayashi, *Bull. Chem. Soc. Jpn.* **2004**, *77*, 13; b) T. Hayashi, K. Yamasaki, *Chem. Rev.* **2003**, *103*, 2829; c) K. Fagnou, M. Lautens, *Chem. Rev.* **2003**, *103*, 169; d) C. Bolm, J. P. Hildebrand, K. Muñiz, N. Hermanns, *Angew. Chem.* **2001**, *113*, 3382; *Angew. Chem. Int. Ed.* **2001**, *40*, 3284; e) T. Hayashi, *Synlett* **2001**, 879.

[5] For its mechanism, see: T. Hayashi, M. Takahashi, Y. Takaya, M. Ogasawara, *J. Am. Chem. Soc.* **2002**, *124*, 5052.

[6] T. Hayashi, K. Ueyama, N. Tokunaga, K. Yoshida, *J. Am. Chem. Soc.* **2003**, *125*, 11508.

[7] a) R. Shintani, K. Ueyama, I. Yamada, T. Hayashi, *Org. Lett.* **2004**, *6*, 3425; b) Y. Otomaru, K. Okamoto, R. Shintani, T. Hayashi, *J. Org. Chem.* **2005**, *70*, 2503; c) R. Shintani, T. Kimura, T. Hayashi, *Chem. Commun.* **2005**, 3213; d) T. Hayashi, N. Tokunaga, K. Okamoto, R. Shintani, *Chem. Lett.* **2005**, *34*, 1480; e) R. Shintani, K. Okamoto, T. Hayashi, *Org. Lett.* **2005**, *7*, 4757; f) Y. Otomaru, A. Kina, R. Shintani, T. Hayashi, *Tetrahedron: Asymmetry* **2005**, *16*, 1673; g) A. Kina, K. Ueyama, T. Hayashi, *Org. Lett.* **2005**, *7*, 5889.

[8] a) C. Fischer, C. Defieber, T. Suzuki, E. M. Carreira, *J. Am. Chem. Soc.* **2004**, *126*, 1628; b) C. Defieber, J.-F. Paquin, S. Serna, E. M. Carreira, *Org. Lett.* **2004**, *6*, 3873; c) J.-F. Paquin, C. Defieber, C. R. J. Stephenson, E. M. Carreira, *J. Am. Chem. Soc.* **2005**, *127*, 10850; d) J.-F. Paquin, C. R. J. Stephenson, C. Defieber, E. M. Carreira, *Org. Lett.* **2005**, *7*, 3821; e) F. Läng, F. Breher, D. Stein, H. Grützmacher, *Organometallics* **2005**, *24*, 2997.

[9] a) N. Tokunaga, Y. Otomaru, K. Okamoto, K. Ueyama, R. Shintani, T. Hayashi, *J. Am. Chem. Soc.* **2004**, *126*, 13584; b) Y. Otomaru, N. Tokunaga, R. Shintani, T. Hayashi, *Org. Lett.* **2005**, *7*, 307; c) T. Nishimura, Y. Yasuhara, T. Hayashi, *Org. Lett.* **2006**, *8*, 979.

[10] a) R. Shintani, K. Okamoto, Y. Otomaru, K. Ueyama, T. Hayashi, *J. Am. Chem. Soc.* **2005**, *127*, 54; b) R. Shintani, A. Tsurusaki, K. Okamoto, T. Hayashi, *Angew. Chem.* **2005**, *117*, 3977; *Angew. Chem. Int. Ed.* **2005**, *44*, 3909; c) R. Shintani, K. Okamoto, T. Hayashi, *Chem. Lett.* **2005**, *34*, 1294.

[11] F.-X. Chen, A. Kina, T. Hayashi, *Org. Lett.* **2006**, *8*, 341.

[12] A. Kina, H. Iwamura, T. Hayashi, *J. Am. Chem. Soc.* **2006**, *128*, 3904.

[13] R. Uson, L. A. Oro, J. A. Cabeza, *Inorg. Synth.* **1985**, *23*, 126.

[14] R. Itooka, Y. Iguchi, N. Miyaura, *J. Org. Chem.* **2003**, *68*, 6000.

[15] In the experiments, phenylboroxine ($(\text{PhBO})_3$) was used as a precursor of **1**; see reference [12].

[16] An excess of boric acid was added to minimize the change in its concentration throughout the reaction.

[17] For an expert review, see: D. G. Blackmond, *Angew. Chem.* **2005**, *117*, 4374; *Angew. Chem. Int. Ed.* **2005**, *44*, 4302.

[18] a) T. Rosner, J. Le Bars, A. Pfaltz, D. G. Blackmond, *J. Am. Chem. Soc.* **2001**, *123*, 1848; b) U. K. Singh, E. R. Strieter, D. G. Blackmond, S. L. Buchwald, *J. Am. Chem. Soc.* **2002**, *124*, 14104; c) S. P. Mathew, S. Gunathilagan, S. M. Roberts, D. G. Blackmond, *Org. Lett.* **2005**, *7*, 4847.

[19] For the parameter ["excess"], see reference [17].

[20] According to Equation (2), the reaction order with respect to Rh_{total} lies between 0.5 and 1, with its value changing with $[\text{Rh}]_{\text{total}}$. Because the concentration of **4** used for the present kinetic studies (1.30–2.76 mM Rh) is lower than that of $[\text{Rh(OH)(binap)}]_2$ (8.00–16.0 mM Rh), the apparent reaction order with respect to Rh_{total} becomes larger (0.65) than 0.5, which was observed for the binap catalyst. The half-order kinetics with respect to the catalyst is reported in references [12] and [18a].

[21] Kinetic modeling of the data to fit the proposed rate expression was carried out with the Excel Solver program. Error analysis of the fits was performed with SlovStat (a statistics program purchased with E. J. Billo, *Excel for Chemists*, Wiley, New York, **2001**).

Received: June 9, 2006